Research Article | Vol. 26, No. 7 | 2 Apr 2018 | OPTICS EXPRESS 8418
Optics EXPRESS

# Amplifier-free 200-Gb/s tandem SSB doubly differential QPSK signal transmission over 80-km SSMF with simplified receiver-side DSP

TINGTING ZHANG,* CHRISTIAN SANCHEZ, STYLIANOS SYGLETOS, IAN PHILLIPS, AND ANDREW ELLIS

*Aston Institute of Photonic Technologies (AIPT), Aston University, Birmingham, B4 7ET, UK*
**zhangt16@aston.ac.uk*

**Abstract:** We numerically demonstrate 80-km standard single-mode fiber transmission without optical amplification, dispersion compensation or carrier recovery using 200-Gb/s tandem single sideband modulated doubly differential QPSK. Simulation results show that doubly differential encoding enables practically constant system performance for frequency offsets within ± 2.3 GHz and allows a linewidth tolerance of $2.5 \times 10^{-3}$ at 1-dB receiver sensitivity penalty. Employing 2.9-MHz linewidth lasers, the receiver sensitivity penalty at 7% HD-FEC threshold for 80-km transmission is less than 0.2 dB. By adding a 12-symbol decision feedback in the 2nd differential operation of doubly differential decoding, the receiver sensitivity is improved by 3.7 dB.



**OCIS codes:** (060.2330) Fiber optics communications; (060.4080) Modulation.

## References and links

1. T. Takahara, T. Tanaka, M. Nishihara, Y. Kai, L. Li, Z. Tao, and J. Rasmussen, "Discrete Multi-Tone for 100 Gb/s Optical Access Networks," in *Proc. OFC* (2014), paper M2I.1.
2. K. P. Zhong, X. Zhou, Y. L. Gao, W. Chen, J. W. Man, L. Zeng, A. P. T. Lau, and C. Lu, "140-Gb/s 20-km Transmission of PAM-4 Signal at 1.3 μm for Short Reach Communications," IEEE Photonics Technol. Lett. **27**(16), 1757–1760 (2015).
3. X. Chen, C. Antonelli, S. Chandrasekhar, G. Raybon, J. sinsky, A. Mecozzi, M. Shtaif, and P. Winzer, "218-Gb/s Single-Wavelength, Single-Polarization, Single-Photodiode Transmission Over 125-km of Standard Singlemode Fiber Using Kramers-Kronig Detection," in Proc. OFC, paper Th5B.6 (2017).
4. S. T. Le, K. Schuh, M. Chagnon, F. Buchali, R. Dischler, V. Aref, H. Buelow, and K. Engenhardt, "8x256Gbps Virtual-Carrier Assisted WDM Direct-Detection Transmission over a Single Span of 200km," in *Proc. ECOC* (2017), paper Th.PDP.B.1.
5. A. Mecozzi, C. Antonelli, and M. Shtaif, "Kramers–Kronig coherent receiver," Optica **3**(11), 1220–1227 (2016).
6. Z. Li, M. S. Erkilinc, K. Shi, E. Sillenkens, L. Galdino, B. C. Thomsen, P. Bayvel, and R. I. Killey, "Joint optimization of resampling rate and carrier-to-signal power ratio in direct-detection Kramers-Kronig receivers," in Proc. ECOC, paper W.2.D.3 (2017).
7. H. Chien and J. Yu, "On single-carrier 400G line side optics using PM-256QAM," in *Proc. ECOC* (2016).
8. P. J. Winzer, A. H. Gnauck, S. Chandrasekhar, S. Draving, J. Evangelista, and B. Zhu, "Generation and 1,200-km transmission of 448-Gb/s ETDM 56-Gbaud PDM 16-QAM using a single I/Q modulator," in *Proc. ECOC* (2010).
9. X. Liu, S. Chandrasekhar, B. Zhu, P. J. Winzer, A. H. Gnauck, and D. W. Peckham, "448-Gb/s Reduced-Guard-Interval CO-OFDM Transmission Over 2000 km of Ultra-Large-Area Fiber and Five 80-GHz-Grid ROADMs," J. Lightwave Technol. **29**(4), 483–490 (2011).
10. M. S. Erkılınç, D. Lavery, K. Shi, B. C. Thomsen, R. I. Killey, S. J. Savory, and P. Bayvel, "Bidirectional Wavelength-Division Multiplexing Transmission Over Installed Fibre Using a Simplified Optical Coherent Access Transceiver," Nat. Commun. **8**(1), 1043 (2017).
11. T. T. Zhang, C. Sanchez, I. Phillips, S. Sygletos, and A. D. Ellis, "200-Gb/s Polarization Multiplexed Doubly Differential QPSK Signal Transmission over 80-km SSMF Using Tandem SSB without Optical Amplification," in *Proc. ECOC* (2017), paper P1.SC4.69.
12. A. Narasimha, X. J. Meng, M. C. Wu, and E. Yablonovitch, "Tandem single sideband modulation scheme for doubling spectral efficiency of analogue fibre links," Electron. Lett. **36**(13), 1135–1136 (2000).

#309756 https://doi.org/10.1364/OE.26.008418
Journal © 2018 Received 23 Oct 2017; revised 9 Feb 2018; accepted 13 Feb 2018; published 23 Mar 2018

Optics EXPRESS

13. A. J. Walsh, J. Mountjoy, H. Shams, A. Fagan, A. D. Ellis, and L. P. Barry, "Highly Robust Dual-Polarization Doubly Differential PSK Coherent Optical Packet Receiver for Energy Efficient Reconfigurable Networks," J. Lightwave Technol. **33**(24), 5218–5226 (2015).
14. N. Sigron, I. Tselniker, and M. Nazarathy, "Carrier phase estimation for optically coherent QPSK based on Wiener-optimal and adaptive Multi-Symbol Delay Detection (MSDD)," Opt. Express **20**(3), 1981–2003 (2012).
15. Y. Wang, K. Shi, and E. Serpedi, "Non-Data-Aided Feedforward Carrier Frequency Offset Estimators for QAM Constellations: A Nonlinear Least-Squares Approach," EURASIP J. Adv. Sig. Pr. **13**, 1993–2001 (2004).
16. A. Viterbi, "Nonlinear estimation of PSK-modulated carrier phase with application to burst digital transmission," IEEE Trans. Inf. Theory **29**(4), 543–551 (1983).
17. C. R. S. Fludger, T. Duthel, D. Borne, C. Schulien, E. Schmidt, T. Wuth, J. Geyer, E. Man, G. Khoe, and H. Waardt, "Coherent Equalization and POLMUX-RZ-DQPSK for Robust 100-GE Transmission," J. Lightwave Technol. **26**(1), 64–72 (2008).
18. D. K. Alphen and W. C. Lindsey, "Higher-order differential phase shift keyed modulation," IEEE Trans. Commun. **42**(234), 440–448 (1994).
19. http://www.markimicrowave.com/Assets/datasheets/QH-0550.pdf.
20. Y. Tang, W. Shieh, and B. S. Krongold, "DFT-Spread OFDM for Fiber Nonlinearity Mitigation," IEEE Photonics Technol. Lett. **22**(16), 1250–1252 (2010).
21. P. Poggiolini, A. Nespola, Y. Jiang, G. Bosco, A. Carena, L. Bertignono, S. M. Bilal, S. Abrate, and F. Forghieri, "Analytical and Experimental Results on System Maximum Reach Increase Through Symbol Rate Optimization," J. Lightwave Technol. **34**(8), 1872–1885 (2016).
22. A. Ellis, A. K. Mishra, P. Frascella, I. Tomkos, S. K. Ibrahim, J. Zhao, and F. C. G. Gunning, "Adaptive modulation schemes," in *Proc. IEEE/LEOS Topical Meeting* (2009), paper TUD3.2.
23. A. D. Ellis, "DSP-lite Coherent Transmission," presented at OFC Workshop "Does analog photonics have a role in a digital world", USA, 18th March 2013.
24. https://www.ntt-electronics.com/en/news/2016/3/industry-first-16nm-100g-200g-coherent-dsp.html.
25. R. Schmogrow, S. Ben-Ezra, P. Schindler, B. Nebendahl, C. Koos, W. Freude, and J. Leuthold, "Pulse Shaping With Digital, Electrical, and Optical Filters—A Comparison," J. Lightwave Technol. **31**(15), 2570–2577 (2013).
26. http://www.microlambdawireless.com/uploads/files/pdfs/MLTO%20Series%20TO-8%20Wideband%20Data%20Sheet.pdf.
27. http://www.markimicrowave.com/Assets/datasheets/ADM-0126-5835SM.pdf.
28. https://nardamiteq.com/viewmodel.php?model=SYS3X3842.
29. http://www.fujitsu.com/downloads/MICRO/fma/pdf/56G_ADC_FactSheet.pdf.

## 1. Introduction

Direct detection systems using direct modulation and advanced modulation formats [1,2] have been widely investigated for 100-Gb/s data center interconnection (DCI), where cost and power consumption are critical. Due to the bandwidth limitation of directly modulated lasers and dispersion limits, external modulation [3,4] direct detection systems utilizing Kramers-Kronig (KK) receivers [5] have been proposed for future DCI. In KK solutions, a powerful digital signal processing (DSP) algorithm (KK scheme) with either a high sampling rate (≥3 Samples/symbol) [6] or iterative processing [5] is required to suppress signal-signal beating interference and ensure acceptable system performance. Optical amplification is also often required to meet power budget requirements [3–6]. Despite increased optical system complexity, coherent solutions [7–9] fundamentally achieve higher capacity due to the ready access to all four field dimensions and longer system reach with significantly improved noise performance. Coherent detection also enables the omission of optical amplifiers in high loss systems such as high-split-ratio passive optical networks [10]. However, challenges for coherent solutions remain to reduce DSP complexity and improve energy efficiency for high order modulation formats. Therefore, alternative solutions, which minimize DSP whilst offering high receiver sensitivity and enabling optical amplifier-free operation, would be attractive.

In this paper, we propose and numerically demonstrate a polarization division multiplexed and subcarrier multiplexed coherent system with a net bit rate of 200 Gb/s (216-Gb/s gross bit rate) using doubly differential (DD) quadrature phase shift keying (QPSK) for 80-km fiber transmission. The system is designed to operate without optical amplification, dispersion compensation or carrier recovery, and we recently reported [11] that this can be enabled by resorting to three key technologies. Firstly, tandem single sideband (TSSB) modulation [12] makes full use of the available opto-electronic bandwidth, allowing independent signals to be

Optics EXPRESS

carried on the upper and lower sidebands, thus doubling the transponder capacity with regard to single sideband (SSB) modulation. Secondly, subcarrier multiplexing (SCM) provides dispersion tolerance, allowing dispersion compensation to be avoided from the DSP stack. Finally, DD encoding [13] eliminates the requirement for carrier recovery including frequency offset (FO) estimation and phase noise compensation, greatly simplifying the DSP. In this paper, we provide further details of the results presented in [11], including discussion of the underlying principles of DD encoding, and the FO as well as linewidth tolerance of DDQPSK with respect to QPSK. We also introduce a fourth technology, multi-symbol decision feedback, to effectively improve the receiver sensitivity in DDQPSK system and evaluate the potential power consumption savings enabled by DD encoding.

Our specific numerical results demonstrate that FOs within ± 2.3 GHz have negligible impact on system performance at 7% hard-decision forward error correction (HD-FEC) threshold for bit-error-rate (BER) of $3.8 \times 10^{-3}$. A combined-linewidth symbol-duration product of $2.5 \times 10^{-3}$ at 1-dB receiver sensitivity penalty has been achieved thanks to DD encoding. Employing 2.9-MHz linewidth lasers with FOs up to ± 2.3 GHz results in a receiver sensitivity below –25.4 dBm at 7% FEC threshold after 80-km transmission with less than 0.2-dB transmission penalty. By including 13-tap multi-symbol decision feedback [14] with unity tap weights in the 2nd differential stage, the receiver sensitivity is improved by 3.7 dB.

## 2. Principles of operation

### *2.1 Doubly differential coding*

Coherent receivers offer the advantage of high receiver sensitivity at the cost of increased complexity due to the requirement for frequency and phase synchronization. However, DSP algorithms used for carrier recovery with free-running local oscillators have limited FO and linewidth tolerance. For example, the FO estimation range in QPSK systems employing a fast Fourier transform (FFT) algorithm [15] or a Viterbi-Viterbi (VV) algorithm [16] is limited to ± B/8 because of the inherent 4th power operation, where B refers to the symbol rate. Furthermore, the susceptibility to cycle slips leads to continuous errors in all following symbols unless differential logical detection (DLD) [17] is implemented, with the consequence of doubled BER. Alternative DSP algorithms may alleviate these disadvantages to a limited extent, but the DSP complexity still remains. DD encoding automatically mitigates FO and phase noise effects, bypassing the requirement for carrier recovery in conventional coherent systems. The complexity of digital carrier recovery is replaced by two simple logic operations in the transmitter and receiver, which consequently reduces the receiver-side DSP complexity.

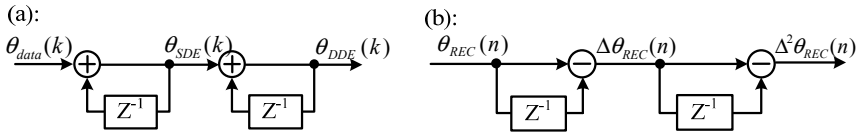


Fig. 1. Principle of (a) DD precoding and (b) DD decoding.

Optics EXPRESS

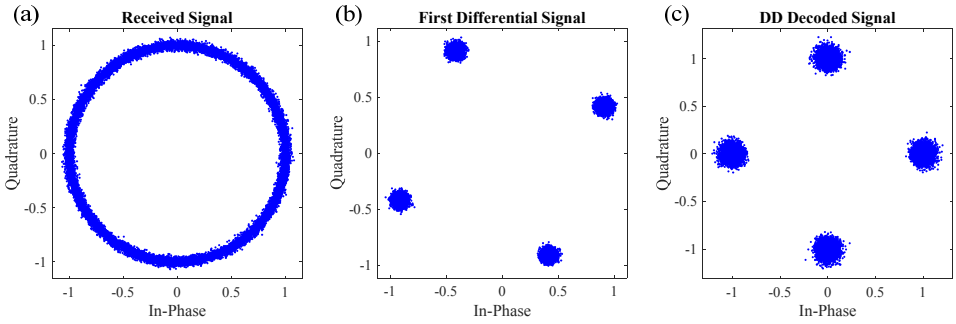


Fig. 2. Constellations of (a) the received ( $\theta_{REC}$ ), (b) first differential ( $\Delta\theta_{REC}$ ) and (c) DD decoded ( $\Delta^2\theta_{REC}$ ) signals in Fig. 1(b).

To implement doubly differential encoding, the phase of a Gray-coded QPSK signal is differentially pre-coded twice in the transmitter, as depicted in Fig. 1(a). Following this operation, the generated DDQPSK signal can be expressed as [18]:

$$\theta_{DDE}(k) = \theta_{data}(k) + 2\theta_{DDE}(k-1) - \theta_{DDE}(k-2) \mod 2\pi,\ k \geq 3 \tag{1}$$

Here, $k$ is the symbol index, while $\theta_{data}$ and $\theta_{DDE}$ refer to the phase of the Gray-coded QPSK and DDQPSK signals respectively. As shown in Fig. 1(b), the decoding scheme can be simply realized utilizing two consecutive differential operations. For a coherent system with unknown FO and phase noise, the detected signal, which typically has a noisy circular constellation [e.g. Figure 2(a)], can be written as:

$$\theta_{REC}(n) = \theta_{DDE}(n) + n\omega_{OF}T_s + \varphi_p(n) \tag{2}$$

Here, $\theta_{REC}$ refers to the received signal's phase with both FO ( $\omega_{OF}$ ) and phase noise ( $\varphi_p$ ) taken into account; $n$ and $T_s$ denote the index of the received signal and the symbol-duration time respectively. In the case of slowly changing phase noise, the signal's phase after the 1st differential operation becomes:

$$\Delta\theta_{REC}(n) = \theta_{DDE}(n) - \theta_{DDE}(n-1) + \omega_{OF}T_s = \theta_{SDE}(n) + \omega_{OF}T_s \tag{3}$$

Here, $\theta_{SDE}$ corresponds to the signal phase after the 1st differential precoding in the transmitter. Equation (3) shows that the 1st differential operation simultaneously mitigates the impact of phase noise and converts FO into a phase offset, as depicted in the constellation of Fig. 2(b). Figure 2(c) demonstrates that, similar to conventional differential QPSK (DQPSK), this phase offset corresponding to the residual constellation rotation ( $\omega_{OF}T_s$ ) can be easily removed after the 2nd differential operation. This can be verified by calculating the signal after the 2nd differential demodulation:

$$\Delta^2\theta_{REC} = \Delta\theta_{REC}(n) - \Delta\theta_{REC}(n-1) = \theta_{SDE}(n) - \theta_{SDE}(n-1) = \theta_{data}(n) \tag{4}$$

We can see that both FO and phase noise have been eliminated after DD decoding. Note that the differential operations in both DDQPSK and DQPSK systems are implemented before the final symbol decision, which cause theoretical penalties of 7.17 dB and 2.4 dB with respect to a QPSK system respectively [13]. By contrast, in QPSK systems with DLD to avoid cycle slips, the differential operation is carried out after symbol decisions, thus the noise enhancement is replaced with BER doubling.

Optics EXPRESS

### 2.2 Tandem single sideband modulation

If an in-phase quadrature (IQ) modulator, consisting of two Mach-Zehnder modulators with a tunable phase difference, is driven by a signal with its Hilbert transform, SSB signal can be obtained when the optical phase shift is equal to 90°. A suitable Hilbert transform for the drive signal can be achieved using a conventional single-input 90 degree hybrid, which generates 90° phase shift between the signals at its two output ports. If a 2 × 2 90 degree hybrid is employed with two separate input signals, coupled signals with 90 degree phase shifts between their output components are generated. Independent upper and lower sideband signals can be also achieved through digital signal processing (e.g. applying a Hilbert transform to each data signal with appropriate digital signal combinations). However, in order to minimize the transmitter power consumption, we implement our Hilbert transforms and signal combinations with passive four-port 90 degree electrical hybrids in the RF domain. Assuming that the two electrical SCM signals input to different input ports (Port 1 and 2) of the 2 × 2 hybrid are written as:

$$S_{1,\text{in}}(t) = I_1(t)\cos\omega_1 t - Q_1(t)\sin\omega_1 t \tag{5}$$

$$S_{2,\text{in}}(t) = I_2(t)\cos\omega_2 t - Q_2(t)\sin\omega_2 t \tag{6}$$

where $I_i(t)$ and $Q_i(t)$ are the real and imaginary information at time $t$ carried by the $i^{th}$ ($i = 1, 2$) subcarrier with angular frequency of $\omega_i$. The sub-modulators are biased at their null points with a 90° optical phase shift in between (IQ operation). Utilizing a small signal approximation and following a simple derivation, the output signal can be expressed as:

$$E'(t) = -\frac{1}{2}A\beta\left\{j\left[I_1(t) + jQ_1(t)\right]e^{j(\omega_c+\omega_1)t} + \left[I_2(t) - jQ_2(t)\right]e^{j(\omega_c-\omega_2)t}\right\} \tag{7}$$

where $A$ and $\omega_c$ are the amplitude and angular frequency of the optical carrier, and $\beta$ represents the modulation index. Equation (7) shows the single sideband up-conversion of the data from Port 1 of the hybrid to the upper sideband (USB), and the data from Port 2 to the lower sideband (LSB). Commercially available 90 degree hybrids commonly have an imperfect phase difference and amplitude imbalance at two output ports, which induces a finite suppression ratio (the power ratio between the desired SSB signal and its image about the optical carrier). As the same subcarrier frequencies are employed in our scheme for both sidebands, appropriate suppression ratio is required to ensure good system performance, considering the inter-subcarrier interference caused by the sideband image. In section 4.1, we verify that the penalty caused by the imperfection of typical commercially available hybrids [19] is below 1 dB.

### 2.3 Subcarrier multiplexing optimization

The number and frequencies of the radio frequency (RF) subcarriers were decided by trading off the dispersion tolerance, available opto-electronic hardware bandwidth and system cost. Firstly, for a net bit rate of 200 Gb/s (excluding 7% FEC overhead) TSSB dual-polarization QPSK system without guard band nor Nyquist pulse shaping, the required total electrical bandwidth is ~27 GHz ($200_{\text{Gb/s}}\cdot(1 + 0.07)/2_{\text{polarizations}}/2_{\text{sidebands}}/2_{\text{bits/symbol}}$). However, for TSSB DDQPSK system when frequency offsets between the transmitter and receiver lasers are expected, guard bands between subcarriers are required to minimize inter-subcarrier crosstalk, given that the detected SCM DDQPSK signal is down-converted and low-pass filtered before DD decoding. To achieve FO tolerance of ± 2.3 GHz in our case, guard bands around 4 GHz were included between subcarriers. The use of guard bands biases the design to the smallest number of RF subcarriers in order to realize high spectral density.

Optics EXPRESS

On the other hand, as the dispersion penalties are proportional to the square of the symbol rate per subcarrier, a larger number of subcarriers would be favored to reduce dispersion impact. Restricting the maximum electrical bandwidth to 45 GHz, and allowing for high pass response of commercially available 90 degree hybrids, a configuration with three RF subcarriers (symbol rate of 9 Gbaud/s per carrier) was adopted for TSSB signal generation. In addition, to minimize system cost, an integer relationship of the RF subcarriers' frequencies (13 GHz, 26 GHz and 39 GHz) was selected, which could be readily implemented with frequency multipliers. In this paper, the SCM parameters have been optimized to minimize the equalization requirements in an 80-km transmission system. However, we note that a similar configuration with different subcarrier spacing and symbol rate, optimized to enhance nonlinear transmission performance [20–22], could be used for long-haul transmission.

## 3. Simulation setup

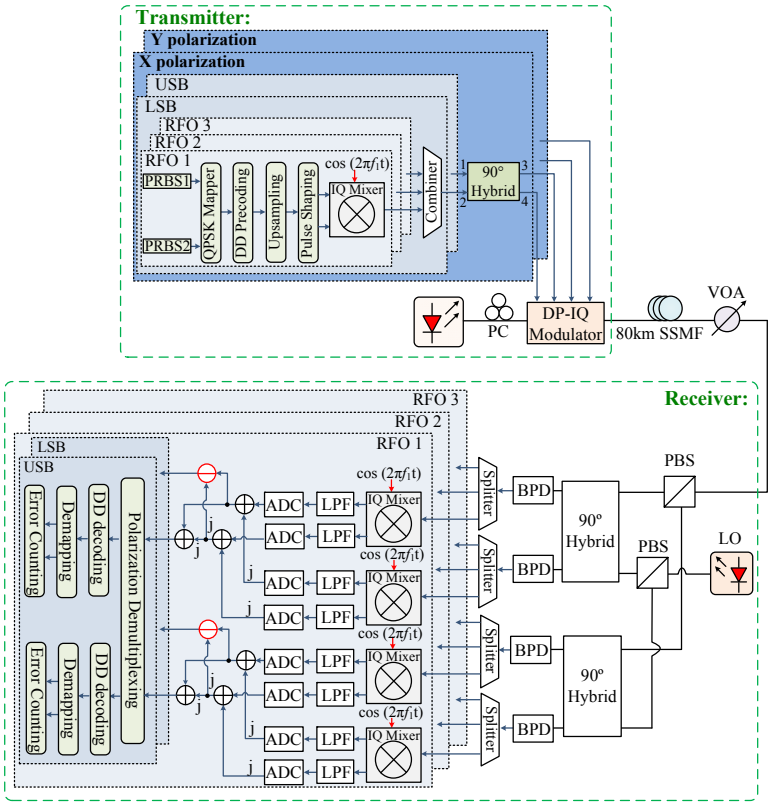


Fig. 3. Simulation setup of the proposed 200-Gb/s TSSB DDQPSK system. PC: polarization controller; VOA: variable optical attenuator; PBS: polarization beam splitter; BPD: balanced photo-detector; LPF: low-pass filter; ADC: analogue-to-digital converter. Green dashed boxes enclose the transmitter and receiver, whilst the black dotted boxes enclose digital and RF signal processing.

The simulation setup for the proposed TSSB DDQPSK system, with a net bit rate of 200 Gb/s (gross bit rate of 216 Gb/s with 7% FEC overhead), is shown in Fig. 3. Matlab cosimulation in VPI TransmissionMaker V9.8 and Matlab were utilized for digital and RF signal processing, whilst opto-electronic conversion and optical propagation were simulated in VPI. In the transmitter, two independent $2^7$-1 pseudo random binary sequences (PRBSs) were firstly bit-wise Gray-coded into QPSK signals and then doubly differentially pre-coded to generate DDQPSK signals, which had symbol rate of 9 Gbaud/s and symbol length of 32768 for each subcarrier per polarization. After being up-sampled to 16 Samples/symbol, the

Optics EXPRESS

generated DDQPSK signals were pulse shaped using square root raised cosine filters with roll-off factor of 0.3 and 3-dB bandwidth of 9.9 GHz. Three RF oscillators (RFOs) with frequencies of 13 GHz, 26 GHz and 39 GHz were employed for signal up-conversion via ideal IQ mixers before the passive combiner. The combined SCM DDQPSK signals (one for the USB and the other for the LSB) were separately sent to two input ports (Port 1 and 2) of an ideal four-port 90 degree hybrid to generate a coupled signal and its Hilbert transform. The same configuration was used for both polarizations and the output signals with power of 5 dBm from two 90 degree hybrids were utilized to drive a dual-polarization (DP) IQ modulator with 5-V half-wave voltage and 6-dB insertion loss. The sub-modulators were biased at their null points with a 90° optical phase shift, and the generated TSSB signal consequently had an output power of −5.6 dBm.

A laser emitting at 193.1 THz with 10-dBm output power was used at the transmitter, while a receiver-side local oscillator (LO) with an output power of 18 dBm was employed without precise frequency control. The coherent receiver also included two PBSs, two 90 degree optical hybrids, and four 43-GHz balanced photodetectors, which had 0.54-A/W responsivity, shot noise and 40-pA/Hz$^{1/2}$ thermal noise current. The detected signal for both polarizations were firstly split into separate down conversion circuits with IQ mixers and RFOs. Since both RFOs and LO may have frequency offsets with respect to those in the transmitter, a quasi-baseband signal was obtained after down-conversion, which was low-pass filtered and then resampled to 2 Samples/symbol using ADCs. The complex information signals carried on LSB and USB were separately obtained utilizing complex adders (as depicted in Fig. 3). Four 7-tap adaptive finite impulse response filters in a butterfly configuration with tap spacing of 55.6 ps and tap weights optimized through constant modulus algorithm were used for polarization de-multiplexing. After DD decoding and de-mapping, the final bit errors were summed over all subcarriers and polarizations, and the average BER and its standard deviation were calculated from ten simulation results per measurement with different random noise seeds. No carrier recovery or chromatic dispersion compensation were carried out in the receiver.

## 4. Simulation results

### *4.1 Impact of hybrid imperfection*

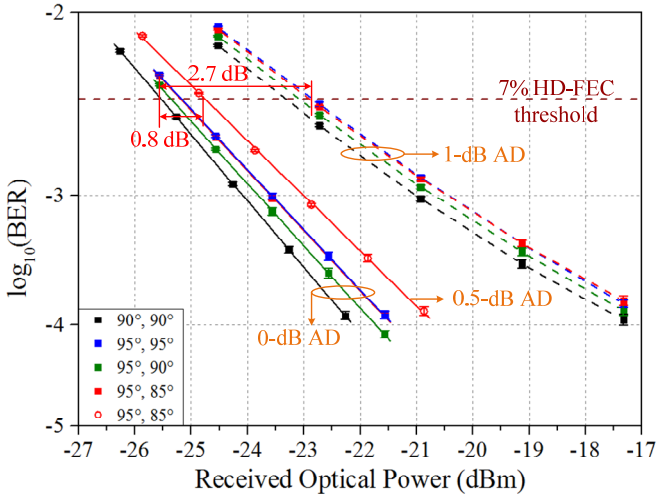


Fig. 4. BER curves for 200-Gb/s TSSB DP-DDQPSK back-to-back system using 2.9-MHz linewidth lasers with ideal or imperfect 90 degree hybrids at zero FO. The phase differences between the signal and its phase shifted copy at two output ports, for signals input to port 1 and 2 of the hybrid are represented in the legend (different colors for different phase condition). AD: amplitude difference.

Optics EXPRESS

Employing the simulation setup described in the last section, we investigated the performance of a 200-Gb/s TSSB DDQPSK back-to-back system at zero FO, using ideal hybrids or commercially available 90 degree hybrids [19] with the specified maximum amplitude difference of 1 dB and phase imperfection of 5° between two output ports, both separately and simultaneously. Figure 4 shows that phase imperfection at both two output ports ([95°, 85°] and [95°, 95°]) for the same amplitude difference only results in a 0.5-dB sensitivity penalty at the 7% FEC threshold. By contrast, the performance is degraded by 2.2 dB for a 1-dB AD under all phase conditions, indicating that the system performance is more sensitive to the amplitude imbalance than to the phase imperfection. For hybrids with both 1-dB AD and 5° phase imperfection, the receiver sensitivity is 2.7 dB away from that using ideal hybrids. These results show that the amplitude balance of the 90 degree hybrid is critical to the system performance.

### *4.2 Frequency offset and linewidth tolerance*

We studied the performance of the 200-Gb/s DDQPSK back-to-back system using 100-kHz lasers for different FOs. To allow for fully asynchronous operation, we tuned the frequency of the 1st RFO in the receiver to have maximum FO of ± 100 MHz with respect to that in the transmitter, leading to a maximum RFO-induced FO of ± 300 MHz for the 3rd subcarrier due to frequency multiplication. Simultaneously, we also changed the frequency of the LO to introduce an LO-induced FO of ± 2 GHz, commensurate with the specifications of commercial integrated tunable lasers. Figure 5(a) shows that without carrier recovery, the 200-Gb/s DDQPSK system performance remains practically constant for LO-induced FO within ± 2 GHz at received power of −22.9 dBm, irrespective of RFO detuning. The simulated BER was varied between $1.5 \times 10^{-4}$ and $2 \times 10^{-4}$ for an overall FO (combining both LO and RFO) range of 4.6 GHz ( ± 2.3 GHz), indicating good FO tolerance. For FOs outside this range, the performance degraded with the increment of FO, owing to bandwidth limitation of the low-pass filter and the increasing inter subcarrier crosstalk caused by leakage of a neighboring channel through the low-pass filter.

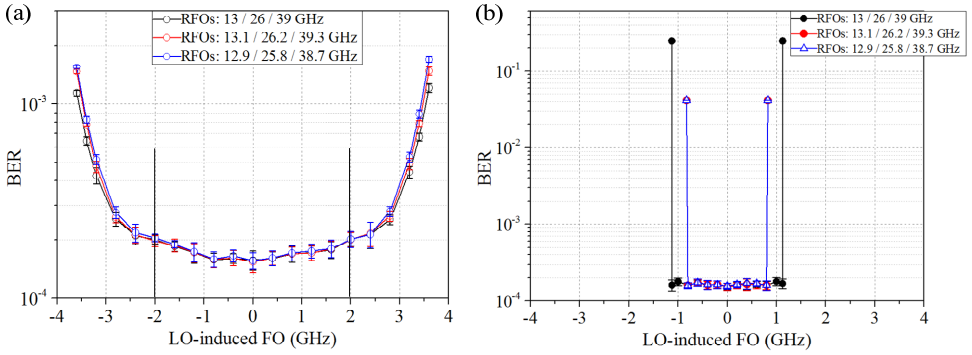


Fig. 5. Back-to-back performance of (a) the 200-Gb/s DDQPSK system without carrier recovery at −22.9-dBm received power and (b) the 200-Gb/s QPSK system with carrier recovery at −30.1-dBm received power by changing frequencies of LO and the receiver-side RLOs (shown in legend).

In the 200-Gb/s QPSK system, the DD pre-coder in the proposed transmitter was eliminated, and the DD decoding in the proposed receiver was replaced by an FFT-based algorithm for FO estimation and conventional VV algorithm for phase recovery. Figure 5(b) shows that at received power of −30.1 dBm (giving roughly the same BER as DDQPSK system at zero FO), the tolerable FO in QPSK system is below ± 1.12 GHz, in line with theoretical expectation ( ± B/8, B = 9 Gbaud/s in our system). In the case of RFO detuning, the outermost subcarrier channel suffered the most, thus the tolerable LO-induced FO is 300-

Optics EXPRESS

MHz smaller than that without RFO detuning. Comparing Fig. 5(a) with 5(b), we can see that DD encoding cannot only simplify the receiver-side DSP by avoiding carrier recovery, but can also double the tolerable FO range. As both LO and RFO detuning result in the residual FO of the down-converted signals, for simplicity, we assume zero RFO-induced FO and emulate the FO (within ± 2.3 GHz) by tuning the LO frequency in the remainder of this paper.

The linewidth tolerance for both systems was also evaluated by setting the overall FO to be zero and employing lasers with the same linewidths in the transmitter and receiver. The linewidth tolerance was defined as the combined linewidth symbol duration product at 1-dB receiver sensitivity penalty, compared to that at the 7% HD-FEC threshold with zero linewidth. To mitigate cycle slips for QPSK, a differential pre-coder after Gray coding was included in the transmitter with post decision differential decoding implemented in the receiver. The VV block size in the QPSK system was optimized for each linewidth. As shown in Fig. 6, the normalized linewidth tolerance for QPSK is $1.5 \times 10^{-3}$, whilst for DDQPSK without carrier recovery, the tolerance is increased by ~67% to $2.5 \times 10^{-3}$.

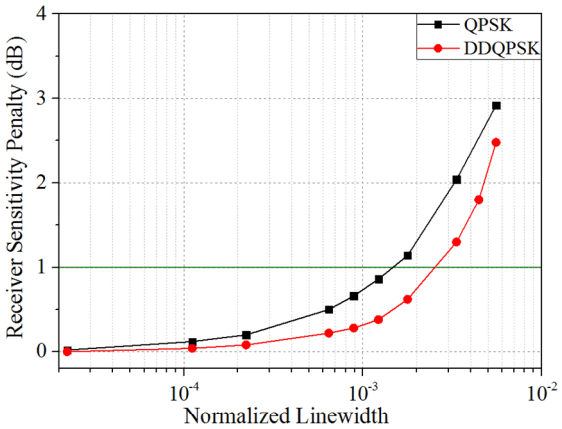


Fig. 6. Linewidth tolerance for 200-Gb/s DDQPSK without carrier recovery and QPSK using VV algorithm with optimal block size for phase noise compensation at zero FO.

### *4.3 Receiver sensitivity of the 200-Gb/s DDQPSK system*

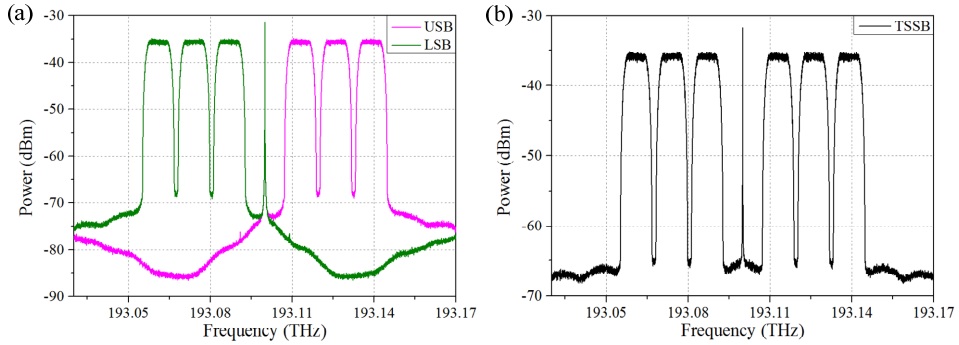


Fig. 7. Optical spectrum of the generated (a) SSB (USB or LSB) and (b) TSSB DDQPSK signal before transmission.

Figure 7(a) shows the optical spectrum of the SSB modulated SCM-DDQPSK signal before transmission, where only the LSB or USB signal was generated with the symmetric one suppressed. By contrast, TSSB modulation, as shown in Fig. 7(b), enables independent signals carried on both the LSB and USB, doubling the system capacity. Figure 8(a) compares

Optics EXPRESS

the back-to-back performance of a 100-Gb/s SSB DDQPSK system, where only the LSB or USB signal was transmitted, with a 200-Gb/s TSSB DDQPSK system at zero FO utilizing laser linewidth of 100 kHz. A 3.2-dB change in receiver sensitivity is observed when both sidebands are transmitted simultaneously, corresponding to a 0.2-dB additional implementation penalty when the capacity increase is taken into account. With 2.9-MHz linewidth lasers, the receiver sensitivity in TSSB system was only degraded by a further 0.2 dB, consistent with the results shown in Fig. 6. Figure 8(b) illustrates that employing 2.9-MHz linewidth lasers even without carrier recovery nor dispersion compensation, the receiver sensitivity at 7% HD-FEC threshold for TSSB DDQPSK transmission over 80-km fiber is below −25.4 dBm with less than 0.2-dB transmission penalty. For both back-to-back and 80-km transmission, the system performance is almost immune to the FOs with negligible penalty. In order to ensure that all pattern-dependent effects are taken into account in the model, we also simulated the 200-Gb/s TSSB DDQPSK signal generated from $2^{15}$-1 PRBSs, transmitted over 80-km fiber with 2.3-GHz FO and 2.9-MHz linewidth lasers. As shown in Fig. 8(b), no performance difference is observed for the different PRBS pattern lengths.

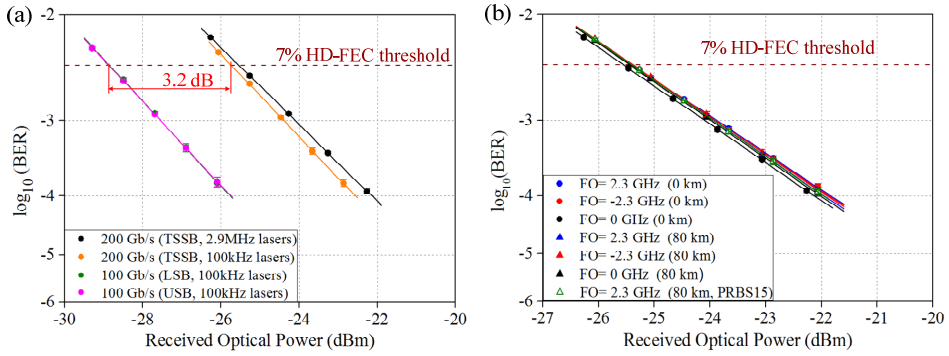


Fig. 8. (a) BER curves of DDQPSK back-to-back system using SSB/TSSB and 2.9-MHz/100-kHz linewidth lasers at zero FO. (b) 200-Gb/s TSSB DDQPSK signal transmission over different fiber lengths (0 km and 80 km) using 2.9-MHz linewidth lasers with varied FO and different PRBS lengths. Only $2^{15}$-1 PRBSs were utilized for the green hollow triangular with $2^{7}$-1 PRBSs used for the other legends.

To investigate the trade-off between system performance and complexity, we numerically studied the back-to-back performance of the 200-Gb/s TSSB system for different modulation formats (QPSK, DLD-assisted QPSK, DQPSK and DDQPSK), as shown in Fig. 9. We assumed zero FO and 100-kHz linewidth lasers for simplicity. Note that the transmitters with single stage differential pre-coding for DQPSK and DLD-assisted QPSK systems were identical. As expected, compared to QPSK without differential logical detection, a penalty of 2.3 dB (theoretically 2.4 dB) is observed for DQPSK due to the differential operation before symbol decision, and 0.7 dB for DLD-assisted QPSK because of doubled errors. For DDQPSK, two consecutive differential operations in DD decoding increase the noise power significantly, resulting in a receiver sensitivity degradation of 7 dB (theoretically 7.17 dB).

Optics EXPRESS

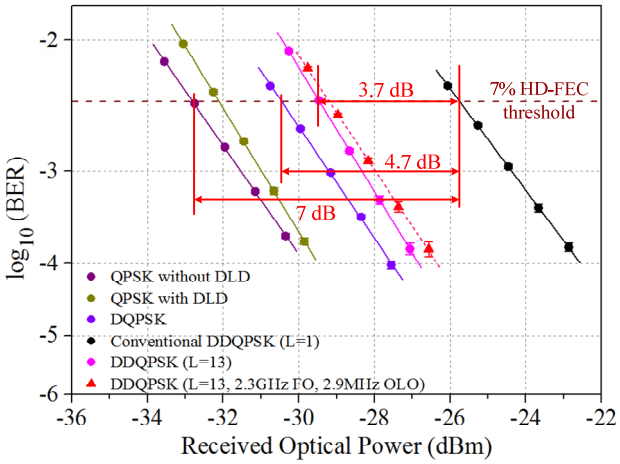


Fig. 9. BER curves of back-to-back system using 100-kHz (circular dots) or 2.9-MHz (triangle) linewidth lasers and QPSK with/without DLD, DQPSK, DDQPSK without (L = 1) or with 12-symbol decision feedback (L = 13) under zero FO (dots, solid line) or 2.3-GHz FO (triangle, dash line).

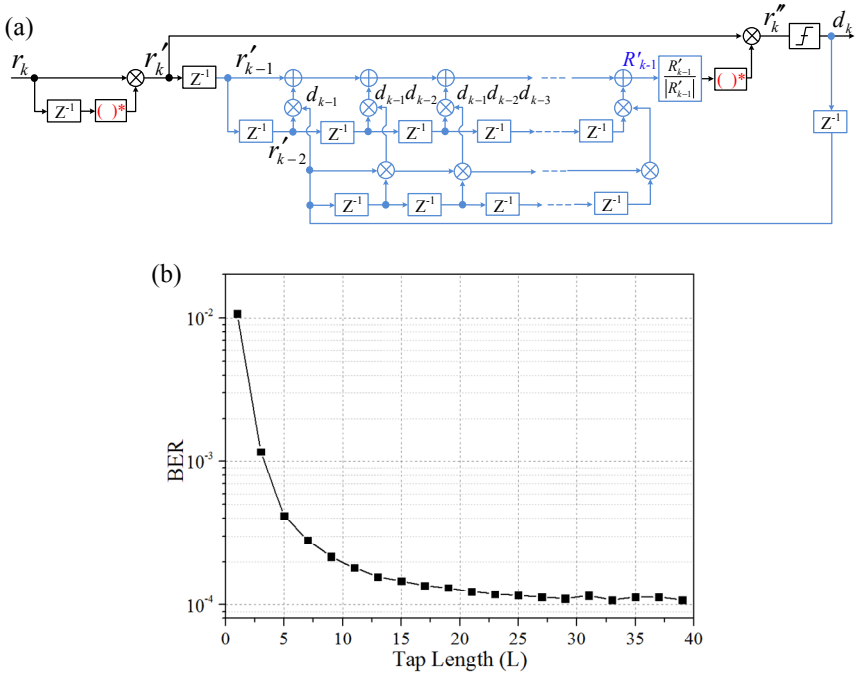


Fig. 10. (a) Block diagram for the DD decoding with multi-symbol decision feedback [14]. (b) 200-Gb/s DDQPSK back-to-back system performance against tap length (L) at –27.1-dBm received power and zero FO with 100-kHz linewidth lasers.

Since the 2nd differential operation results in much larger penalty (4.7 dB) than the 1st one (2.3 dB), we added multi-symbol decision feedback [14] in the 2nd differential stage to effectively suppress the phase noise. Specifically, instead of using one symbol as phase reference for the symbol of interest, several additional consecutive symbols in combination of the factorial of feedback decisions, as depicted in Fig. 10(a), were summed and averaged to generate less noisy phase reference for the 2nd differential operation. The principle of this scheme can be found in [14], where adaptive weights enable better system performance than

Optics EXPRESS

constant weights. However, the decision feedback algorithm with constant weights allows simpler DSP and easier hardware implementation, thus it was adopted in our paper. Figure 10(b) shows that multi-symbol decision feedback (L>1) continuously improves the performance as the tap length (L) increases. BER performance converged after 29 taps for a received power of −27.1 dBm, but a tap length of 13 was adopted in our system to minimize complexity with acceptable receiver sensitivity penalty less than 0.5 dB. With this configuration, the receiver sensitivity at the 7% FEC threshold was improved by 3.7 dB. Furthermore, the net penalty with respect to DLD-assisted QPSK, which would be deployed in practice, was only 2.6 dB (see dark yellow and pink circle dots in Fig. 9). The red triangle symbols in Fig. 9 demonstrate that the advantage of high robustness to FO and phase noise is retained with multi-symbol decision feedback algorithm, and only a 0.3-dB penalty was observed when the laser linewidth was increased to 2.9 MHz and the FO simultaneously increased to 2.3 GHz.

## 5. Power consumption and complexity

As shown in section 4, the proposed twin sideband, subcarrier multiplexed, and doubly differentially modulated system is intended to trade off DSP complexity and performance, offering the elimination of carrier recovery and dispersion compensating blocks at the expense of 7-dB (conventional DDQPSK) or 3.3-dB (with 12-symbol decision feedback) penalties. It was proposed in 2013 that simple subcarrier multiplexing (without TSSB or DD encoding) would offer savings of 64% in power consumption when compared to transponders based on the available DSP chips at the time [23]. However, despite repeated prophecies of doom, complementary metal-oxide-semiconductor (CMOS) technology continues to follow its roadmap, delivering higher levels of integration and lower energy consumption per operation. At the time of writing, published commercial digital coherent receiver application-specific integrated circuits (ASICs) offer performance in the region of 10 W per 100 Gb/s [24], and adding this to the power consumption associated with modulator drivers, lasers, and FEC, gives a total estimated power consumption around 360 pJ/b for a 200-Gb/s digital coherent system.

The energy consumption of the final hardware implementation of the proposed TSSB DDQPSK system was calculated by assuming modulator drivers with the same output swing, the same lasers and FEC. Note that digital to analogue converters are not strictly required in our system, if analogue filters are used for pulse shaping [25], and that the power consumed by additional electrical amplifiers, which are required to compensate for the loss of the filters, mixers and electrical hybrids (all are passive components), is small compared to that of the driver amplifiers. With the power consumption of commercially available RF oscillators [26–28], ADCs [29] and the residual DSP (neither dispersion compensation nor carrier recovery) taken into consideration, the proposed scheme has a predicted energy consumption of about 135 pJ/b. The power consumption advantage of this technique lies in the reduction of digital signal processing, but it is clearly ill-advised to make definitive predictions in the face of continued development of CMOS. However, the maintenance of a 60% energy consumption advantage in the proposed system over digital coherent reception is encouraging.

Compared with digital coherent single-carrier solution, the proposed scheme requires larger electrical bandwidth due to the inclusion of guard bands. The bandwidth overhead depends on the target frequency offset tolerance and the symbol rate (determined by the tolerable dispersion). We believe that the trade-off between this bandwidth increase, the net 2.6-dB sensitivity penalty with respect to digital coherent, and the reduced energy consumption is worthy to consider in deciding whether the proposed technology is suitable for any given application. Although a proof-of-concept demonstration of TSSB DDQPSK system using discrete RF components seems to be complex and bulky, a more compact (and potentially even more energy-efficient) configuration, comprising the combination of an optical and a mixed-signal ASIC could be readily deployed in volume production. Such a

Optics EXPRESS

solution would have a similar cost structure to digital coherent, but would of course be impacted by production volumes.

## 6. Conclusion

In this paper, we have numerically demonstrated a 200-Gb/s TSSB modulated DDQPSK signal transmission over 80-km fiber without optical amplification, dispersion compensation or carrier recovery. DD encoding enables wider FO estimation range and 67% improvement of the linewidth tolerance compared to a QPSK system utilizing FFT and VV algorithms for carrier recovery. The impact of FO (within ± 2.3 GHz) on DDQPSK system performance has also been demonstrated to be negligible. In the case of 2.9-MHz linewidth lasers employed, the receiver sensitivity at 7% HD-FEC threshold for 80-km transmission was below −25.4 dBm with less than 0.2-dB transmission penalty. By including a 12-symbol decision feedback algorithm in the 2$^{nd}$ differential decoding stage, the receiver sensitivity in conventional DDQPSK system is improved by 3.7 dB. Compared with digital coherent system, the proposed scheme is believed to have an energy saving of 60%. In circumstances when the ultimate performance of digital coherent receivers are not required, we believe that this scheme merits careful attention, offering potential power savings in exchange for moderate reduction in performance.

The data underlying this publication can be found at http://doi.org/10.17036/researchdata.aston.ac.uk.00000293.

## Funding

China Scholarship Council (CSC); Engineering and Physical Sciences Research Council projects PEACE (EP/L000091/1), UPON (EP/M005283/1), SPFS (EP/L00044X/1), TOM3 (EP/M009092/1), UNLOC (EP/J017582/1); European Union project INVENTION (659950).